

## High-resolution measurement of the helium $1s2s^2\ ^2S$ resonance profile

R. E. Kennerly, R. J. Van Brunt,\* and A. C. Gallagher†

*Joint Institute for Laboratory Astrophysics, University of Colorado and National Bureau of Standards, Boulder, Colorado 80309*

(Received 9 May 1980)

The 19.37-eV helium scattering resonance profile has been measured with an instrumental width less than the natural width and much less than that attained in any previously published study. The electron beam was produced by photoionization and scattered from a He beam from a supersonic nozzle. The instrumental width, including residual Doppler effects, was routinely around 5 meV and the current was  $5 \times 10^{-12}$  A. The profile was measured at 22°, 90°, and 135° scattering angles. From the 90° and 135° data the *s*- and *p*-wave phase shifts were found to be  $1.813 \pm 0.017$  and  $0.309 \pm 0.013$  radians, respectively. The natural width  $\Gamma$  of the resonance was inferred by two methods: nonlinear least-squares fitting, and use of the integral of the differential cross section over the resonance. Both methods yield  $11.0 \pm 0.5$  meV, if it is assumed that there is no instrumental background in the scattered electron signal. Experimental evidence indicates that any such instrumental background must be less than 15% of the total signal, and is probably less than 5%. If an extreme allowance is made for the larger figure, a  $\Gamma$  as high as 13 meV could be possible.

### I. INTRODUCTION

The helium ( $1s2s^2\ ^2S$ ) resonance at 19.37 eV was the first Feshbach resonance to be observed in electron-atom scattering,<sup>1</sup> and has since been the object of considerable experimental and theoretical investigation. Reviews of earlier work have been given by Schulz,<sup>2</sup> Golden,<sup>3</sup> and Andrick.<sup>4</sup> A chronological depiction of previous experimental and theoretical values for the *s*-wave phase shift ( $\eta_0$ ) at the resonance energy, and for the natural width ( $\Gamma$ ) of the resonance, is shown in Figs. 1 and 2. As can be seen, the theories generally agree within a few percent on  $\eta_0$ , while the experimental results are more widely scattered and generally higher. In the case of  $\Gamma$  the majority of the experiments, and particularly the three claiming the greatest accuracy, disagree with all but one of 14 calculations.

The phase shift can be inferred from measurements of the elastic scattering angular distribution above and below the resonance energy (boxes in Fig. 1), while  $\eta_0$  and  $\Gamma$  can also be inferred from analysis of the resonance profile. However, in all previous experiments the instrumental width  $\omega$  considerably exceeded  $\Gamma$ , so that the actual resonance profile was not observed.  $\Gamma$  values have thus been obtained from these experiments using arguments regarding the fractional area under the observed resonance profile, and  $\eta_0$  values are obtained from the asymmetry of the observed resonance. A variety of possible systematic uncertainties in such measurements are eliminated if  $\omega \ll \Gamma$  so that a close approximation to the resonance profile is observed. This has been largely achieved in the present experiment, in which  $\omega = 4\text{--}7$  meV compared to  $\Gamma \cong 11$  meV. (About 2 meV of this instrumental width is due to

the electron beam and the remainder is residual Doppler width.) This resolution has allowed a more complete and definitive diagnosis of the resonance profile, resulting we believe in a more accurate determination of  $\eta_0$  and particularly of  $\Gamma$ .

To achieve the desired level of resolution and accuracy has required considerable time in development, measurements, and analysis, but the results are quite gratifying. Our  $\eta_0$  result is in excellent agreement with very thorough recent angular distribution measurements by Willaims and Willis and with very sophisticated recent calculations (and several others). Also in contrast to the previous situation, our measured  $\Gamma$  value agrees with many of the calculations, particularly most of the very elaborate ones. Furthermore, we believe that we have identified a subtle potential source of systematic error that could explain some low experimental values for  $\Gamma$  from other experiments.

### II. APPARATUS

The experimental arrangement is similar to that previously described,<sup>5</sup> although several modifications have been made for the present measurements.<sup>6,7</sup> A diagram of the apparatus is shown in Fig. 3. Electrons are produced in the source chamber by near-threshold photoionization of a beam containing metastable Ba atoms. The ionization occurs inside a field-free region within the cavity of a cw He-Cd ultraviolet laser. The laser operated at 3250 Å provides sufficient photon energy to produce electrons with an initial kinetic energy of 17 meV via photoionization of barium atoms excited in a discharge to the  $^1D_2$  metastable state (see Fig. 3). Electrons leaving

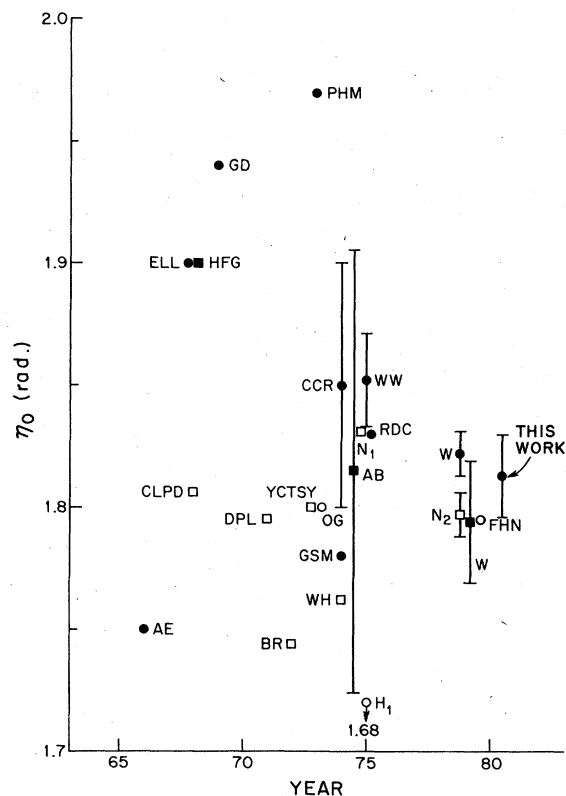


FIG. 1. Published results for the  $s$ -wave direct elastic scattering phase shift at or near the  $^2S$  resonance energy versus year. Experimental results are indicated by closed figures and theoretical by open figures. Results derived from studies of the direct scattering are indicated by boxes and those derived from resonant scattering by circles. The letters near the plotted values are the initials of the authors. The references are as follows: AE (Ref. 37), CLPD (45), ELL (38), HFG (46), GD (36), DPL (47), BR (48), YCTSY (49), OG (50), PHM (25), WH (51), GSM (28), CCR (27), AB (15),  $N_1$  (52), WW (30), RDC (29),  $H_1$  (53), W (14),  $N_2$  (16), and FHN (17). The meaning of the error bars is given in the text.

the source are accelerated and focused by an electrostatic lens system onto a second atomic beam from which scattering occurs. In the present arrangement elastically scattered electrons are collected by detection systems fixed at 22, 90, and 135° scattering angles. Electron-beam current is monitored with an electron multiplier. Electron-beam currents up to  $1 \times 10^{-11}$  A have been achieved. The source chamber, electron optics, and entire scattering chamber are constructed of molybdenum to reduce effects of non-uniformities and contact potentials. The components were cleaned by an acid etching procedure (Mo-1 of Ref. 8) selected for its lack of reaction products remaining on cleaned surfaces. Electrons in the scattering region have an energy

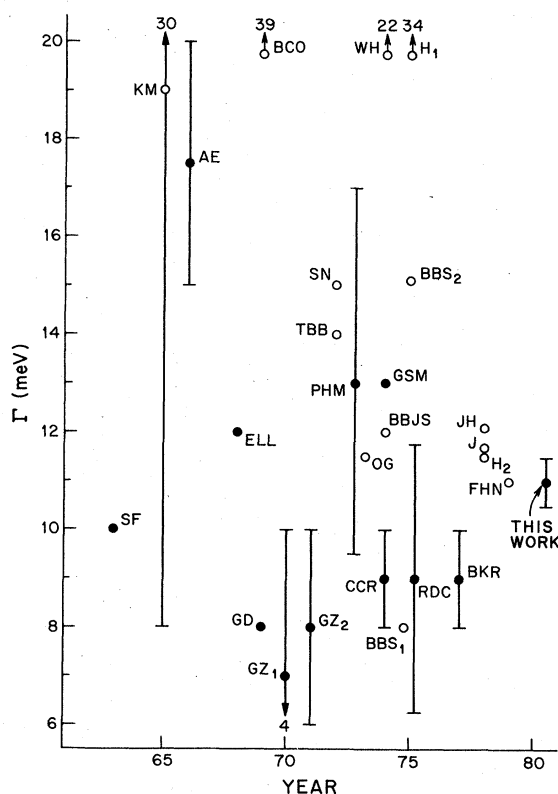


FIG. 2. Published results for the natural width of the  $^2S$  resonance. Symbols are the same as in Fig. 1. References not given in the caption to Fig. 1 are SF (34), KM (54), BCO (55),  $GZ_1$  (56),  $GZ_2$  (35), SN (21), TBB (57), BBS<sub>1</sub> (58), BBS<sub>2</sub> (60), BKR (9),  $H_2$  (40), JH (41), and J (42).

$E_e = (0.017 + V + C)$  eV, where  $V$  is the potential difference between the electron source and scattering chamber and  $C$  is the contact-potential shift which was typically  $\sim 0.03$  eV for the helium measurements.

The supersonic target beam was produced by a nozzle-skimmer arrangement and had a measured full width at half maximum (FWHM) in the range  $\theta = 0.1$ – $0.2$  rad depending largely on nozzle pressure. The system had three differentially pumped volumes: the region between the supersonic nozzle and skimmer, the scattering chamber, and the main chamber containing electron source, electron optics, and detectors. The pressure in the scattering chamber was about 10 times greater than that of the main chamber, which was maintained at  $\leq 1 \times 10^{-6}$  Torr when the atomic beam was on. The ratio of supersonic beam density to thermal background gas density in the scattering volume viewed by the detectors was measured to be about 3 for helium. The base pressure of the entire system was  $\sim 10^{-8}$  Torr. The electron

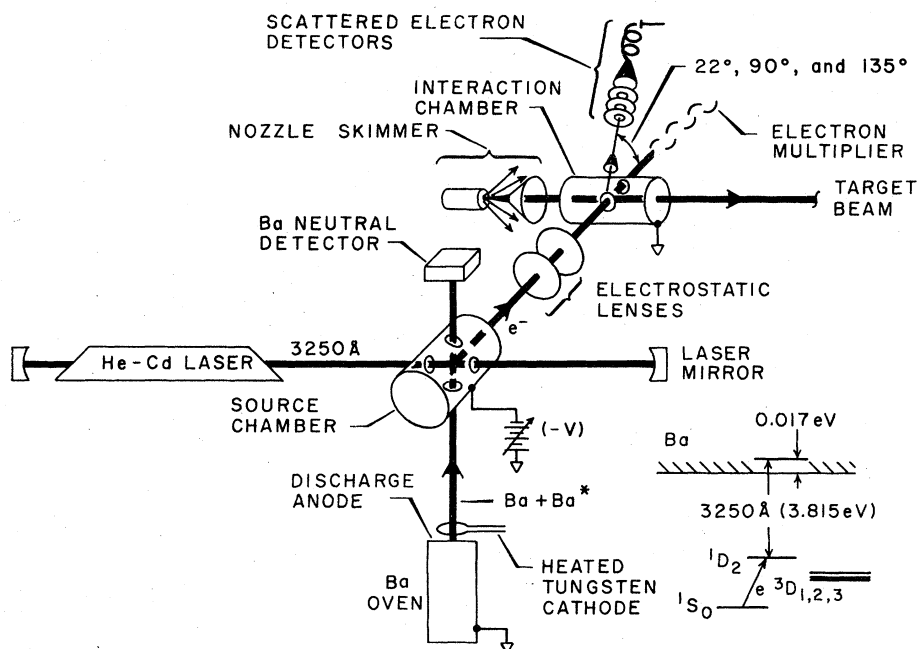


FIG. 3. Experimental arrangement and barium energy levels with indicated relevant excitation and ionization transitions for electron production.

source, the nozzle and skimmer region, and the scattering chamber can be locally baked.

The detectors were channel electron multipliers preceded by shielded three-element lens systems which viewed the scattering volume through a molybdenum mesh 1.6 cm from the scattering volume. The detection optics, the first element of which was strongly retarding, focused a volume of variable size onto a 1-mm aperture behind which was the multiplier. The object space at the electron beam was from 2 to 5 mm in diameter, depending on the electron optical mode used. The acceptance angle was estimated to be about  $\pm 5^\circ$ . Helmholtz coils were used to cancel the ambient magnetic field, typically to  $\sim 30$  mG.

An approximate energy width of the electron source was inferred from observations of resonances believed to be narrow. This is not unambiguous because the overall instrumental width obtained can be much higher than the source width due to Doppler broadening from the target gas beam and background gas, and possibly from stray fields in the scattering region. At one point, the nozzle system was replaced by a gas cell, for which the Doppler broadening is known.<sup>11</sup> The 11.1-eV argon resonance was then observed in differential scattering with the full-Doppler linewidth of 7 meV, indicating that the source width is probably less than 2 meV. Using the nozzle beam, linewidths of 5–6 meV were seen for the  $^2P_{3/2}$  11.1-eV argon resonance and the 11.48-eV

resonance of  $N_2$ , for which the estimated natural widths are 2.5 and 0.6 meV, respectively.<sup>9,10</sup> However, a large portion of this observed width was due to the contribution of background gas which has the full-Doppler width. For the purposes of fitting data from beam-gas scattering, the instrumental width has been considered to be a free parameter. For helium, values from 4–7 meV were found from this fitting, excluding the contribution from background gas (see Sec. IV). (The Doppler width for scattering from background gas was assumed to be the 28 meV for 19.37-eV electrons scattered from He gas at room temperature.) From measurements of the gas-beam angular distribution (full angle at half-height  $\approx 0.15$  rad), it was estimated that the residual Doppler width for scattering from the gas beam should be 3–5 meV. Thus both the argon cell and helium beam measurements were consistent with an electron source width of  $\lesssim 2$  meV.

### III. DATA

The measurement was controlled by a minicomputer programmed to operate as a multichannel scaler. The acceleration voltage was supplied by a high-precision programmable power supply. The accumulation time per channel was such that the integrated electron-beam current per channel was constant. Typical dwell times were around 10 sec/channel. This allowed scans to be com-

pleted in times for which energy scale drifts were insignificant. Such drifts were steady and monotonic, with a rate of about 5 meV/h initially (following the turn on of the electron beam), dropping to about 2 meV/h after several hours. This drift did, however, preclude simply summing repeated scans without adjusting the energy scale. This was accomplished by recording the results of each scan on magnetic tape, and later summing by using some nonsubjective method for assessing the energy shifts. For helium, we chose to find the centroid of the resonance peaks at 90 and 135° for each scan, average the shifts implied at the two angles, round to the nearest whole channel (the channel width was 2 meV), shift, and sum. Since the shifts were always less than 1 meV and averaged only 0.5 meV or  $\frac{1}{4}$  channel, a value very

much less than the observed resonance widths; this method of signal averaging was assumed to have negligible effect on the results. As explained below, no attempt was made to determine the resonance energy absolutely.

Runs lasted from 20–30 h and were usually terminated because of declining laser power due to contamination of the intracavity Brewster window at the vacuum wall. The data from two such runs were used in the analysis described below. Data set 1 (Fig. 4) is the sum of all 20 scans in the run, and set 2 (Fig. 5) is the sum of 27 of 30, three being excluded because of obvious malfunctions during these scans. In these data sets, some data were taken far from the resonance on both the high- and low-energy sides as a check on possible slopes or curvature due to

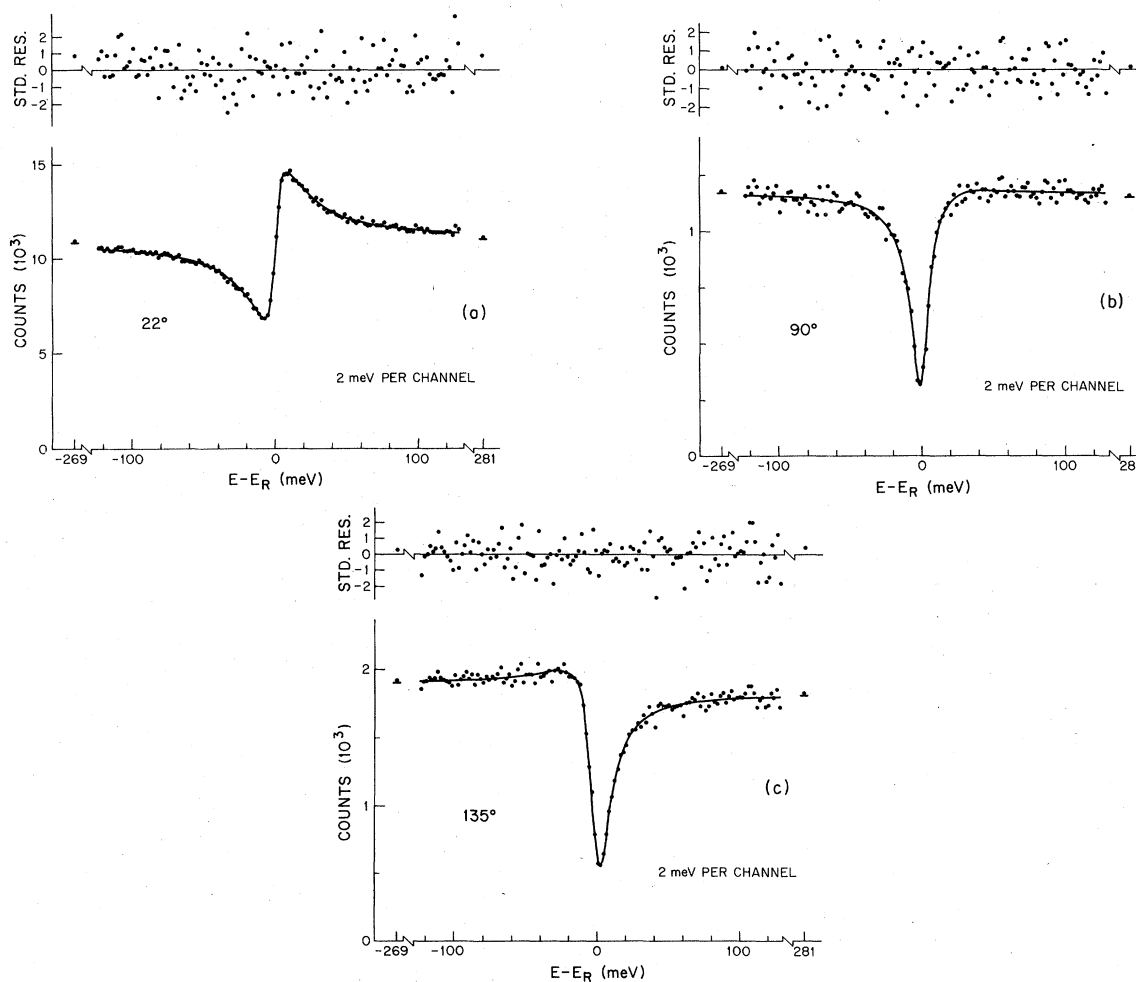


FIG. 4. Data set 1 and fits used in the present analysis. The ordinates are shown unbroken with their actual zeroes. The solid curves are the fits using Eq. (5). Plotted on the upper abscissa are the "standard" residuals (STD. RES.), i.e., the residuals divided by the square root of the number of counts in that channel. The upper ordinate is therefore the number of statistical standard deviations by which the data and fit differ at each point. The zero of the abscissas is at the position determined from the fits.

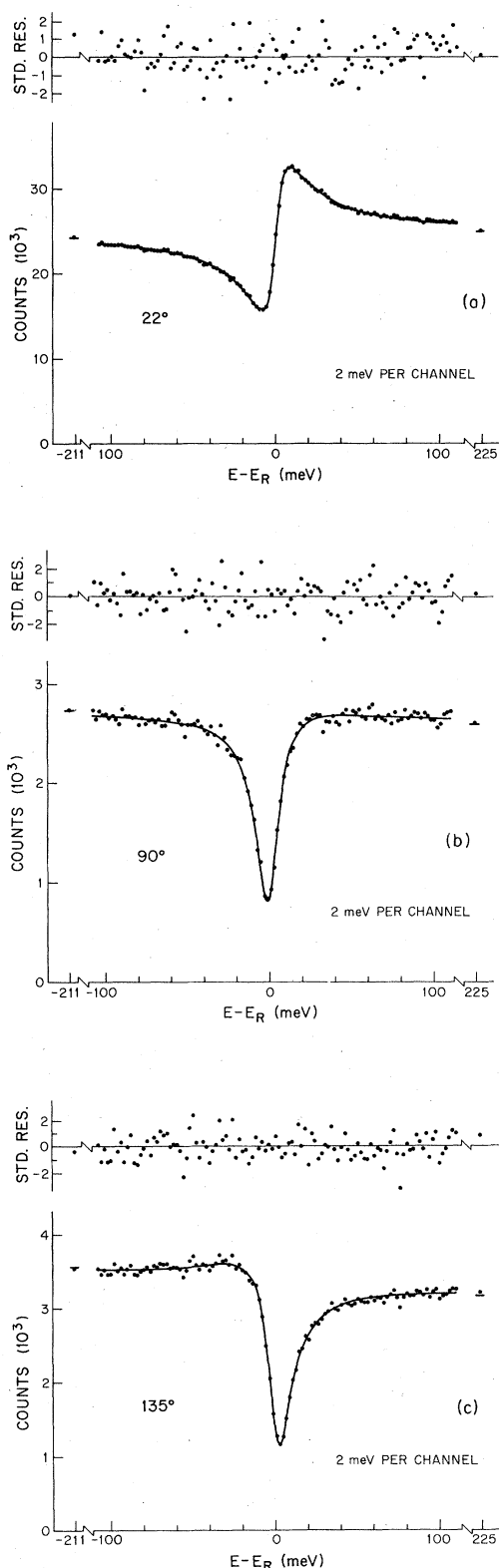


FIG. 5. Data set 2 and fits. (The explanation is the same as for Fig. 4.)

changes in electron optical conditions as the voltage was scanned. These groups consisted of five points separated from the main group by about 0.14 eV in set 1 and 0.10 eV in set 2, and recorded in the same way as those in the main group. The averages of these isolated groups are shown in Figs. 4 and 5 were included with the appropriate weight in all fits.

It was decided that fixing the resonance energy by observation of very narrow threshold features was unlikely to improve on the accuracy of recent experimental results<sup>9</sup> due to the relatively low scattered signal level in the present work, even though our resolution was better. We therefore used a relative energy scale in Figs. 4 and 5. Counting rates at 19 eV were about 20–100, 2–10, and 3–15 Hz, respectively, at the 22, 90, and 135° angles, the range determined by the range of magnifications used in the detection optics and the gas-beam intensity. Two magnifications with a ratio of five were commonly used. Profiles measured at lower magnification differed from that at higher magnification in that they were about 15% broader and the signal was several times as large. Since the lower magnification encompassed a larger gas-beam angle and resulted in a smaller beam- to background-gas density ratio, this is consistent with the finding that the observed peak widths had a substantial full-Doppler contribution.

#### IV. ANALYSIS

The analysis was based on the usual partial-wave formulation of elastic scattering<sup>12</sup> in which the direct scattering amplitude is given by

$$f(k, \theta) = \frac{1}{2ik} \sum_{l=0}^{\infty} (2l+1) (\exp 2i\eta_l - 1) P_l(\cos \theta), \quad (1)$$

where  $k$  is the electron momentum,  $\theta$  is the scattering angle,  $P_l$  is a Legendre polynomial, and the  $\eta_l$  are direct-scattering phase shifts. Near a resonance, the  $\eta_l$  of the resonant angular momentum channel (of index  $l$ ) must be replaced in Eq. (1) by

$$\eta_l^{res} = \eta_l - \arctan\left(\frac{\Gamma/2}{E - E_R}\right), \quad (2)$$

where  $\Gamma$  is the natural width and  $E_R$  is the energy of the resonance.<sup>13</sup> Since the He(1s2s<sup>2</sup>) resonance occurs in the  $s$  wave (i.e.,  $l=0$ ),  $\eta_0^{res}$  from Eq. (2) was used in Eq. (1) for the present work. (The symbol  $\eta_l$  in this paper will be used only for the direct or nonresonant scattering phase shifts.)

Over a sufficiently small energy range, the  $\eta_l$  can be considered constant. This assumption is justified in the present case in which the typical

changes in the  $\eta_l$  over the observed energy range are much less than the final uncertainties assigned to the  $\eta_l$  derived from the fitting. As a check, a fit was made in which the  $\eta_0$  and  $\eta_1$  were linear functions of the energy, with slopes  $-0.015$  and  $0.006$  rad/eV respectively, as suggested by recent studies.<sup>14-17</sup> The resulting  $\eta_0$  differed by only about 0.03% from that derived by assuming  $\eta_0$  and  $\eta_1$  constant.

At low energies the first several partial waves dominate and the higher phase shifts can be approximated. This is commonly done by terminating the sum in (1) at index  $L$  and adding the Born-Thompson<sup>18</sup> expression for the amplitude from all higher  $l$ , given by

$$f(l > L) = \pi \alpha k \left[ \frac{1}{3} - \frac{1}{2} \sin\left(\frac{\theta}{2}\right) - \sum_{l=1}^L \frac{P_l(\cos\theta)}{(2l+3)(2l-1)} \right], \quad (3)$$

where  $\alpha$  is the dipole polarizability 1.384 a.u.<sup>19</sup> This expression follows from assuming a long-range potential of the form  $\alpha/r^4$ . Alternatively one can approximate the higher phase shifts explicitly<sup>20</sup> for use in (1) by

$$\eta_l = \arctan\left(\frac{\pi \alpha k^2}{(2l-1)(2l+1)(2l+3)}\right), \quad (4)$$

and summing to large values of  $L$ , and perhaps using (3) as well. For the present analysis, which uses data for large scattering angles (90 and 135°), these formulations produced identical results.

It has been shown that  $\eta_2$  is very well approximated by (4) for the calculation of differential cross sections.<sup>14,15,21</sup> We therefore assumed that for  $l \geq 2$ , the amplitude was given by one of the above Born formulations; typically, we used  $\eta_2$  from Eq. (4) as the last term in Eq. (1), and Eq. (3) with  $L=2$  for all higher terms. The lack of dependence on the formulation was checked by also using  $\eta_3$  from Eq. (4) and using Eq. (3) with  $L=3$  for all higher terms. The  $\eta_0$  implied by the fitting procedure for the 90° profile was unchanged to nine significant figures. The dependence of the results for  $\eta_0$  and  $\eta_1$  on the assumed  $\eta_2$  is discussed later. As is usual we have ignored the very small contributions of higher-order induced moments to the Born terms.

The resonance line shape implied by (1)-(4) is Lorentzian in character and can be described by two parameters, the width  $\Gamma$  and a "line-shape" or asymmetry parameter.<sup>13</sup> The latter is a function of all the unknown phase shifts, and the problem of obtaining two phase shifts from the asymmetry parameter is thus underdetermined for a profile at one scattering angle. The relative depth of the profile and/or the absolute value of the nonresonant cross section are two additional

pieces of information that can, in principle, also be used in the determination of the unknown phase shifts. However, the presence of broadening effects and the possibility of a nonnegligible background counting level due to electron scattering from surfaces introduces a strong correlation between the broadening and width parameters and the phase shift, if the relative depth of the profile is used in the determination of the phase shift. To avoid this, we have used the angular distribution of the profile shape as the additional information. Since  $P_1=0$  at 90°,  $\eta_1$  has no influence on a profile at 90° and the line-shape or asymmetry parameter is a function of  $\eta_0$  only (since  $\eta_{l>1}$  were assumed known). Using this  $\eta_0$ , we then fit the profile at another angle (in this case 135°) to get  $\eta_1$ .

Because of uncertainties in the gas- and electron-beam profiles, the "effective" scattering angle viewed by the very low angle detector at 22° was uncertain. Since the line-shape parameter depends on the scattering angle, data from this detector were not used in the phase-shift determination. However, as an informative exercise the nominally 22° data were fit by varying the effective scattering angle rather than the phase shifts, which were fixed at the values obtained from the higher angle data. The result was, for both data sets, an effective or average scattering angle of about 18°. This shift from 22° is attributed to the broad atomic beam, the large background-gas density, the forward peaking of the cross section, and the nearness of the detection optics to the scattering region. A much smaller difference between the nominal and effective angle is expected for the 135° data, due to the smaller region of overlap of the electron beam and collection volume. No difference is expected for the 90° data, due to symmetry. The difficulty encountered by Van Brunt and Gallagher<sup>6,7</sup> in fitting earlier 22° detector data is attributed largely to this problem, which was aggravated by a higher background-gas density than in the present data due to a lower pumping speed. (By assuming 22° was the average scattering angle, they observed a profile asymmetry which appeared to be inconsistent with accepted values for the phase shifts.)

The fitting was done using nonlinear least-squares minimization with the Marquardt algorithm.<sup>22</sup> The model profile  $I(E)$  used was

$$I(E) = a_1 + a_2 [1 + a_3(E - \bar{E})] \times \left( a_4 \int \sigma(\eta, E_R, \Gamma; \epsilon) G(\omega; \epsilon - E) d\epsilon + (1 - a_4) \int \sigma(\eta, E_R, \Gamma; \epsilon) G(W; \epsilon - E) d\epsilon \right). \quad (5)$$

In this expression  $\sigma = |f|^2$ , the differential cross section implied by Eqs. (1)–(4), with three free parameters:  $\eta$  (representing either  $\eta_0$  or  $\eta_1$ ),  $\Gamma$ , and  $E_R$ . The functions  $G$  were normalized Gaussians of full width  $W$  and  $\omega$ ;  $\omega$  was the instrumental resolution for scattering from beam gas, and  $W$  was that for scattering from thermal background gas.  $W$  was assumed to be the full-Doppler width 28 meV and  $\omega$  was a free parameter.  $a_1$ ,  $a_2$ ,  $a_3$ , and  $a_4$  were treated as free parameters.  $a_1$  represented the possibility of a constant background count rate and is discussed below. Since the measured profiles were relative cross sections, a normalized parameter  $a_2$  was required.  $a_3$  allowed for small “slopes” in the data due to changes in detection efficiency, electron optical conditions, etc., as the energy was changed. In fact,  $a_3$  was always found to be small (at most 4% over the data range), and in addition was not highly correlated with the other parameters.  $a_4$  gave the relative contribution of detected scattering due to the beam gas and background gas.

The use of two convolutions of different widths was necessitated by the low beam- to background-gas density ratio, which was estimated from nozzle calculations and background pressure measurements to be about three under the conditions used for the profile measurements. The energy width for scattering from thermal He background gas is, as discussed above, very broad, and its effect on the profile can be readily distinguished from that caused by increasing either  $\Gamma$  or  $\omega$  (the energy width for scattering from the He beam) above their “true” values. This is illustrated in Fig. 6, which shows a composite profile in which 70% of the signal was due to scattering from the

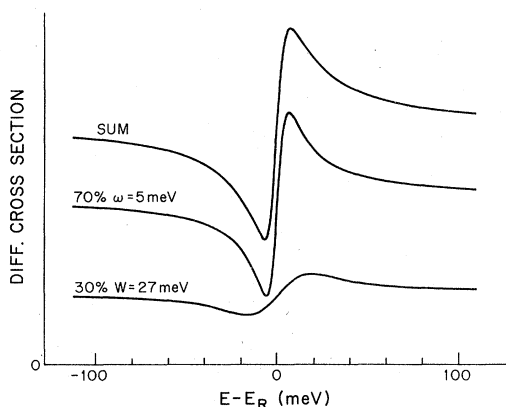


FIG. 6. A composite profile at  $22^\circ$  (similar to those of Fig. 4 and 5) and its two components, illustrating how the presence of a broad (27 meV) underlying component can be distinguished from a “pure” profile with a larger  $\Gamma$  or instrumental width (see text).

He beam and the remainder from the He background gas. Note that the transition from the minimum to the maximum is only very slightly altered by the addition of the broad component, but that the regions near the peaks of the broad component are substantially changed. This change is fundamentally different from that generated by changes in  $\Gamma$  or  $\omega$ . The latter would directly affect the width of the sharp feature, in this case the transition from minimum to maximum. Consequently, the parameters  $a_4$  and  $\Gamma$  or  $\omega$  were not highly correlated in the fitting procedure.

The use of a Gaussian convolution for the background scattering component follows from the fact that Doppler broadening from scattering from a gas with a Maxwellian velocity distribution has a Gaussian profile. [More exactly,  $W$  should be replaced by  $(W^2 + \omega_s^2)^{1/2}$  in Eq. (5), where  $\omega_s$  is the width of the electron energy distribution, but since  $W \geq 15\omega_s$ ,  $W$  alone was adequate.] Since it was found that  $\omega \sim \Gamma/2$ , the assumed form of  $G(\omega)$  was not critical to finding a unique  $\Gamma$ . However, since the phase shifts follow from the symmetry of the resonance profile, a very large asymmetry in the true  $G(\omega)$  not accounted for could possibly affect the determination of the  $\eta$ 's. In the present case,  $G(\omega)$  was itself the convolution of the electron-beam energy profile (at the scattering volume) and the profile due to Doppler broadening from the gas “beam.” As was discussed above, the latter appears to be the major component, and, though perhaps not quite Gaussian, was certainly symmetric. The relative narrowness of the source component  $\approx 2$  meV ensured that if there was some asymmetry here, it had negligible effect on the determination of the phase shifts.

The possibility of a constant background count rate, given in (5) by  $a_1$ , requires some comment. There was no evidence for it at  $90$  and  $135^\circ$ , but it was impossible to prove its total absence. With the gas beam off, the count rates were negligible. However, with gas in the system, electron-atom collisions might have occurred along the length of the electron beam, and slit and surface scattering of these scattered electrons could conceivably have led to a nonnegligible background counting rate at the detectors. An indirect test of  $a_1$  at  $90$  and  $135^\circ$  was made by measuring depth of the resonance profile as a function of He background pressure in the scattering chamber. This pressure was varied (while the gas-beam density was not) by throttling the appropriate diffusion pump. Extrapolation to zero background pressure then removed the contribution from background gas, and using typical values of  $\omega$  and  $\Gamma$ , an upper limit of 5% of the total signal was deduced for the

background counting rate. (Measuring the entire profile with good statistical accuracy as a function of He background pressure would have been prohibitively time consuming.) Support for a low value of the background counting rate at 90 and 135° also arose from analysis of the 22° data. For this scattering angle one would expect a relative background fraction much larger than that at the higher angles because the 22° detection system "looked into" the electron beam and directly viewed some surfaces and an aperture along the beam path. Consistency of the results of the fits for the 22° data with those of the 90 and 135° data required that  $a_1$  at 22° represent 6–10% of the total counting rate. Since we expect this fraction to be at least several times as large as that at the larger angles, this supports an upper limit at 90 and 135° less than or equal to the 5% deduced above. Nevertheless,  $a_1$  was generally allowed to vary freely in our fitting routine. The phase-shift determination was insensitive to this parameter, but the parameters that also determine the depths and widths of the profiles ( $\Gamma$ ,  $\omega$ , and  $a_4$ ) were highly correlated with  $a_1$ . This is discussed further below in connection with the determination of  $\Gamma$ . Starting values of the parameters were obtained from visual comparison of calculated and measured profiles.

The converged values of  $\eta_0$  from data set 1, 90°, was  $1.819 \pm 0.009$  rad, where the uncertainty here is one standard deviation. The reduced  $\chi^2$  was 0.94. Data set 2 yielded  $1.807 \pm 0.008$  rad, with reduced  $\chi^2$  of 1.08. (The  $\chi^2$  values near unity indicate that the model describes the data quite well.) The principal systematic error source was uncertainty in the scattering angle. (An average over the  $\pm 5^\circ$  acceptance angle of the detector produced a negligible change.) Since the entrance aperture was fixed at precisely 90°, the main source of angle uncertainty was possible error in the alignment of the nozzle with respect to the skimmer. Any resulting deviation in effective scattering angle from 90° was probably less than 1°. The change in the derived  $\eta_0$  with change in the assumed effective scattering angle (including the contribution from  $\eta_1$  when  $\theta \neq 90^\circ$ ) was 0.013 rad per degree. The two data sets were taken with identical nozzle-skimmer alignment, so any error from this source would have been the same for both the above  $\eta_0$  values.

The change in the derived  $\eta_0$  for a change in the assumed value of  $\eta_2$  was 2.4 rad per radian. The  $\eta_2$  value used, from Eq. (4), was 0.059. Experimental results<sup>14,15</sup> show no evidence that  $\eta_2$  deviates from Eq. (4) up to about 20 eV, the highest energies studied, and suggest that this approxi-

mation is valid within 5% at the resonance energy. Allowing for such an uncertainty in  $\eta_2$  in our analysis gave a corresponding uncertainty of 0.007 rad in  $\eta_0$ . The  $\eta_0$  values from the two data sets were averaged and the uncertainties and possible errors (which were independent) added in quadrature to give a final value for  $\eta_0$  of  $1.813 \pm 0.017$  rad. Using this value and fitting the 135° data to determine  $\eta_1$ , we obtained  $0.312 \pm 0.004$  rad for data set 1 and  $0.307 \pm 0.004$  rad for set 2, with reduced  $\chi^2$  of 0.85 and 0.89, respectively. Possible error in the 135° scattering angle due to nozzle alignment was less than at 90°, but as noted above a difference between the nominal and the effective angles similar to (but less than) that seen at 22° may have been present. Allowing for possible error of  $\pm 2^\circ$  gave  $\pm 0.006$  in  $\eta_1$ . The uncertainties in  $\eta_1$  due to uncertainty in  $\eta_0$  and  $\eta_2$  were determined by their effects on the  $\eta_1$  values derived from fits; these were  $\pm 0.010$  and  $\pm 0.006$ , respectively. Averaging (as for  $\eta_0$ ) gave a final result for  $\eta_1$  of  $0.307 \pm 0.014$  rad. The fits from which these values were taken are shown in Figs. 4 and 5. Table I lists the relevant parameters derived from fits shown.

The determination of  $\Gamma$  from fits to the data (Table I) was greatly hindered by the relatively large number of parameters in the model which affected the width and/or depth of the profile. As discussed above, the principal culprit was  $a_1$ , which represented the possibility of a background counting rate. This parameter was very highly correlated with  $\Gamma$ , and when allowed to vary freely in the fitting routine, its standard deviation was generally comparable to the value of the parameter itself, which in some cases was negative (a physical impossibility). The large correlation is

TABLE I. Fitting parameters.<sup>a</sup>

(Deg.)	Shape parameter	$\Gamma$ (meV)	$\omega$ (meV)	$a_4$
Data set 1				
22	$\theta = 18.1^\circ$	10.90	5.5	0.60
90	$\eta_0 = 1.819$	10.75	5.2	0.67
135	$\eta_1 = 0.312$	10.44	8.1	0.78
Data set 2				
22	$\theta = 17.2$	14.02	4.98	0.76
90	$\eta_0 = 1.807$	10.74	7.1	0.68
135	$\eta_1 = 0.307$	10.04	7.1	0.64

<sup>a</sup>Parameters from the fits shown in Figs. 4 and 5. In each case it was assumed that  $a_1$ , a constant background counting rate, was zero.  $a_4$  is the fraction of detected electrons scattered from the beam-collimated He gas. See text for a discussion of the fitting model.



due to the fact that, in order to minimize  $\chi^2$ , the dip of the calculated profile must closely match that of the data. A change in  $a_1$  effectively changes the relative profile depth, which can be compensated by changes in  $\Gamma$  and the instrumental width due to their relatively high correlation.

Another method for inferring  $\Gamma$  is to evaluate the area of the profile using the nonresonant intensity as the baseline. This area is proportional to  $\Gamma$  (see Ref. 14) and the proportionality constant, a function of the phase shifts, can be easily derived analytically from (1)–(4). The area is independent of broadening effects, and for nearly symmetric profiles at large scattering angles, like the present ones at 90 and 135°, the error in the proportionality constant due to phase-shift and scattering angle uncertainty is quite small. However, this procedure required that any constant background counting rate (discussed above) be known. If one ignored this, or incorrectly assumed that such a background was zero, then the derived value of  $\Gamma$  would be a lower bound related to the true  $\Gamma$  by  $\Gamma = \Gamma / (1 - F)$ , where  $F$  is the fraction of the total (nonresonant) counting rate which was spurious. ( $F$  is directly related to  $a_1$  of the model.) In the present case, indirect evidence indicated that  $F$  was less than 5% at 90 and 135°, as was discussed above in the section explaining the model used for fitting. Choosing  $F = 0.02$ , a value intermediate between zero and this indirectly deduced upper limit, the value of  $\Gamma$  derived from the area method using the 90 and 135° data was  $11.0 \pm 0.5$  meV. The uncertainty includes the effects of uncertainty in the phase shifts, scattering angles, area determination, and  $F$  value (i.e., background counting rate). This range encompassed the values derived from the least-square fits for the 90 and 135° data when  $a_1$  was fixed at a value corresponding to the above  $F$  value. Since the area method is independent of broadening influences, the consistency of the results from the two methods indicates that the model used in the fitting is a good one.

Although direct demonstration that  $F$  (or  $a_1$ ) was very small was impossible, strict limits on it could be obtained indirectly. The measured profiles had depths (at 90 and 135°) of about 70% of the nonresonant value. The theoretical (unbroadened) profile depths are about 99%. Thus one could rigorously state on this basis that  $F$  could be no larger than 0.30. Moreover, we deduced minimum possible values of the fraction of thermal background gas in the scattering volume (20%) and gas-beam Doppler widths (4 meV), calculated such minimally broadened profiles, compared the profile depths to those of the data, and thereby reduced the range of possible  $F$ . This

procedure gave  $F < 0.15$  and, therefore, a strict upper bound on  $\Gamma$  of 13 meV.

## V. DISCUSSION

The present results of  $\eta_0$ ,  $\eta_1$ , and  $\Gamma$  are shown in Figs. 1, 2, and 6, along with other published values derived from measurements. The figures show error bars where given, but their meaning varies. Some indicate only statistical error while others are more comprehensive. A recent re-analysis<sup>23</sup> of some of these data is not included here. The recent angular distribution measurements of Register *et al.*<sup>24</sup> unfortunately do not report the resulting 19.37-eV phase shifts.

The present value of  $\eta_0$ , the direct scattering  $s$ -wave phase shift at the resonance energy, is in good agreement with most recent experimental results. It is very close to the  $1.815 \pm 5\%$  of Andrick and Bitsch<sup>15</sup> derived from an analysis of relative differential cross sections from a beam-beam measurement. The error quoted there includes some systematic error. The  $\eta_0$  of Preston *et al.*<sup>25</sup> of 1.970 from analysis of the resonance profile in differential scattering from a static gas target is almost certainly much too large. This is also the conclusion of McConkey and Preston,<sup>26</sup> although no explanation was given. The Cvejanovic *et al.*<sup>27</sup> result of  $1.85 \pm 0.05$  derived from the profile at 90° overlaps the present result. The error bars for the former presumably give only the statistical error. The authors assumed that  $\eta_2 = 0.05$  rad. If they had used the Born value (as we did) their  $\eta_0$  would be increased by about 0.04 rad raising it out of agreement with our value. The result of Golden *et al.*<sup>28</sup> of 1.78 was inferred from a fit to the resonance profile in an energy-modulated transmission experiment. Their value, for which no error estimate was given, is outside the present error bars. By comparing calculated profiles to that observed in an unmodulated transmission measurement, Roy *et al.*<sup>29</sup> got 1.83 (with no error estimate) which is at the upper limit of the present result. These authors state that an approximation used in the analysis of Golden *et al.*<sup>28</sup> was not valid and that properly accounting for this would increase the latter's  $\eta_0$  to 1.87, well above the present error limits. This issue has not been investigated here. The results of Williams<sup>14</sup> are from an analysis of the angular dependence of differential elastic scattering ( $1.794 \pm 1.4\%$ ) and from the angular dependence of the profile ( $1.822 \pm 0.5\%$ ). Both agree well with the present value. The error bars shown for this work are largely statistical (one standard deviation) although some systematic effects were included in the first method. The

earlier result by Williams and Willis,<sup>30</sup> with only statistical error bars, is outside the present range, and also outside one of the later results of Williams.<sup>14</sup>

The energy resolution in these measurements was usually around 40–60 meV, including the full-Doppler component in transmission studies. The exception was the work of Roy *et al.*<sup>29</sup> in which the spectrometer resolution of 16 meV combined with the 27-meV Doppler width gave an effective resolution of about 30 meV.

Only recently have theoretical calculations of elastic  $e$ -He scattering included efforts to make estimates of error. The first of these was that of O'Malley *et al.*<sup>31</sup> using the  $R$ -matrix method. Their estimate of probable error for  $\eta_0$  was  $\pm 1/4\%$  above 4 eV, but the highest energy calculated was 16.5 eV. The results of Nesbet<sup>16</sup> also extend only to 16.5 eV but formulas were given allowing extrapolation to the resonance region. The phase shifts implied at 19.365 eV are shown in Figs. 1 and 6. This variational calculation differs from that of Sinfailam and Nesbet<sup>21</sup> principally in that correlated ground-state wave functions were used and a systematic study of convergence with accuracy of the target wave function and the number of states in the close-coupling expansion was made, and estimates of the residual errors were made. The extrapolated  $\eta_0$  was 1.797 with an estimated uncertainty of  $\pm 0.5\%$ , which overlaps the present value. Over their mutual energy range, the  $s$ -wave phase shift from this calculation agree within about  $1/2\%$  with those of O'Malley *et al.*<sup>31</sup> The recent calculations by the linear-algebraic method by Foster *et al.*<sup>17</sup> of near-threshold scattering also included a systematic study of convergence of the  $^2S$  resonance parameters with the level of target wave function and the number of close-coupling states, and error estimates will be made. Their preliminary value for the direct-scattering  $s$ -wave phase shift at the resonance energy was 1.795 rad. The calculated resonance energy was 19.365 eV, in excellent agreement with recent experimental values (see Ref. 9). Their result for the width  $\Gamma$  is given later.

Published results for the  $p$ -wave phase shift at 19.36 eV are shown in Fig. 7. The recent values are in good mutual agreement, and agree well with the present result. As mentioned above, some of the error estimates include only statistical uncertainty. The number of published experimental values for  $\eta_1$  is smaller than that for  $\eta_0$  since transmission methods yield only the direct-scattering phase shift for the resonant partial wave, in this case the  $s$  wave. Also shown is the theoretical result of Nesbet,<sup>16</sup> for which estimated error is much smaller than those of the ex-

periments. This result is within error limits for the present value. In the range of the O'Malley *et al.*<sup>31</sup> calculations (up to 16.5 eV), the Nesbet<sup>16</sup>  $p$ -wave phase shifts are generally several percent larger than the former values (see Fig. 7). The calculations of Foster *et al.*<sup>17</sup> have not yet been extended to  $p$ -wave scattering.

The total nonresonant elastic scattering cross section at 19.36 eV can be calculated from the  $s$ - and  $p$ -wave phase shifts and Born values for the higher ones. The present phase shifts imply  $3.07 \pm 0.05 \text{ \AA}^2$  for this cross section. This is in excellent agreement with the recently measured values near the resonance of  $3.09 (+3, -2\%) \text{ \AA}^2$  of Kennerly and Bonham,<sup>32</sup> and  $3.05 \text{ \AA}^2$  of Stein *et al.*,<sup>33</sup> for which no error estimate was made. The extrapolated phase shifts of Nesbet<sup>16</sup> give  $3.13 \pm 0.03 \text{ \AA}^2$ , which overlaps the present result and that of Kennerly and Bonham.

Published values for the natural width  $\Gamma$  of the resonance are shown in Fig. 2. The variation is much higher than that for the background phase shifts. For the experimental measurements, this presumably is due to the difficulties discus-

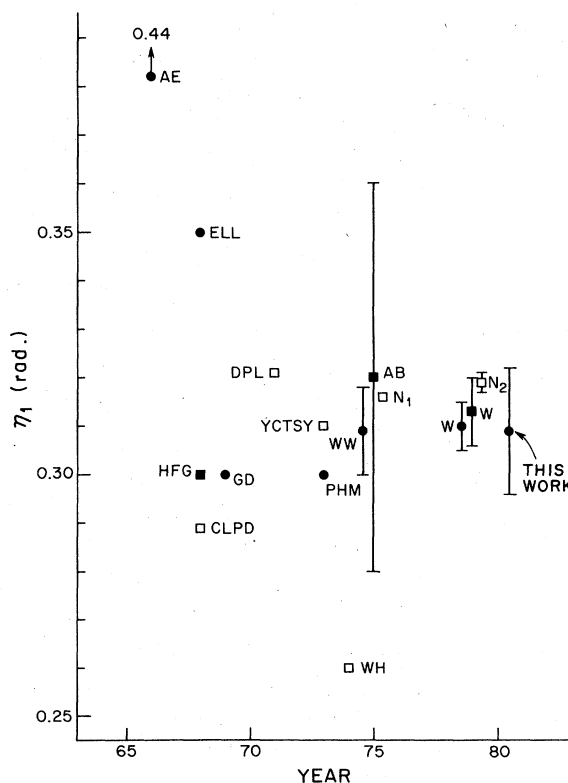


FIG. 7. Published results for the  $p$ -wave direct elastic scattering phase shift at the  $^2S$  resonance energy versus year. Symbols are as in Fig. 1.

sed in the previous section, namely, the lack of sufficiently good and/or well-known instrumental resolution and the uncertainty in background counting rates. Both of these are extremely difficult to determine precisely, but as the resolution is improved the sensitivity to each of these uncertainties decreases. This is the principal advantage of the present  $\Gamma$  determination over previous ones.

The earliest attempt to estimate the width of this resonance was by Simpson and Fano,<sup>34</sup> who studied the profile in transmitted current with energy resolution of about 50 meV. A precise result was not sought and only one significant figure for  $\Gamma$  was reported. The fractional change in the transmitted current at the resonance energy (in analogy to the fractional signal change in differential scattering) cannot be used as a figure of merit unless the pressure and geometry of the scattering cell were given, which is usually not the case. In addition, in all transmission-type measurements the full-Doppler width, in this case about 28 meV, is manifested and since this is about  $2.5\Gamma$ , the sensitivity for evaluating  $\Gamma$  is inherently relatively low. Using an energy-modulated transmission method, Golden and Zecca<sup>35</sup> obtained  $8 \pm 2$  meV for  $\Gamma$  by extrapolation to zero modulation amplitude, and Golden *et al.*<sup>28</sup> obtained 13 meV by matching calculated and measured peak height ratios in the detected signal. The other transmission measurement was that of Roy *et al.*<sup>29</sup> which used conventional electrostatic selectors to achieve resolution of about 30 meV, including the full-Doppler contribution. They deduced about  $9 \text{ meV} \pm 30\%$  for  $\Gamma$ , by comparing calculated and measured profiles and stated that the uncertainty was due in effect to the small value of  $\Gamma$  relative to the Doppler width. Gibson and Dolder<sup>36</sup> examined the resonance profile in differential scattering using a static gas target. At  $90^\circ$  the profile depth was about 20% of the nonresonant signal and a resolution of about 65 meV and a  $\Gamma$  of 8 meV were deduced from least-squares fits. Potentially serious distortions of the measured profiles by attenuation effects not properly cancelled by their current ratio method were not discussed and no error estimate was made. Preston *et al.*<sup>25</sup> describe a similar measurement from which  $\Gamma = 13 \pm 4$  meV was deduced by fitting. The error is presumably statistical only. The profile width at  $85^\circ$  was about 50 meV and the depth was about 12% of the nonresonant signal.

The remainder of the experimental determinations of  $\Gamma$  in Fig. 2 employed a gas-beam target, for which the residual Doppler contribution was smaller, although generally not well known. The resolution quoted in such measurements should

include the Doppler contribution for the gas and electron energy under study, but it is often not clear under what conditions the stated resolution was determined.

The earliest of such gas-beam studies was that of Andrick and Erhardt<sup>37</sup> who estimated  $\Gamma$  to be from 15–20 meV, judging from the 70-meV width and about 20% depth of the  $90^\circ$  profile. (Erhardt *et al.*<sup>38</sup> quote a later unpublished value of 12 meV determined by the above authors using the same methods.) Cvejanović *et al.*<sup>27</sup> used least-squares fits to deduce  $\Gamma = 9 \pm 1$  meV from the  $90^\circ$  profile. The resolution was stated to be 18 meV but the profile width in the exhibited data is about 70 meV and the depth cannot be determined. Brunt *et al.*<sup>9</sup> used the methods of Comer and Read<sup>39</sup> to arrive at  $\Gamma = 9 \pm 1$  meV and an instrumental resolution of  $17 \pm 1$  meV. What model was used and how the error was determined was not given, but the principal source of error was stated to be uncertainty in the background counting rate. The depth of the profile at  $90^\circ$  was 51%. This resolution and depth were the best reported for the study of this resonance prior to the present work. The area method (explained in the previous section) was also used by Brunt *et al.*<sup>9</sup> and implied a value within the uncertainty of the above value of  $\Gamma$ . As was pointed out above, such agreement is to be expected if the same background counting rate is assumed. In all the studies discussed above, this background was assumed to be zero, although no evidence to support this was given and the possibility of its existence has rarely been discussed. To be sure, in a well-designed and well-adjusted apparatus this level can be closely approached. But given the high sensitivity of the inferred  $\Gamma$  to this level, some support for the assumed level seems to be required if error limits around 10% or less are to be achieved. We therefore believe that most of these measurements should be considered to have given lower bounds to  $\Gamma$ . This would account for the tendency of most of these values to lie below the present result and those of recent theoretical studies.

Two recent calculations are within the uncertainty of the present experimental value. Hazi<sup>40</sup> has used an " $L^2$ " method employing Stieltjes-moment theory to deduce a  $\Gamma$  for this resonance of 11.5 meV. The formalism was intended for application to molecules, however, and the author stated that the calculation was not intended to provide highly precise widths for atomic resonances. On the other hand, the calculations of Foster *et al.*<sup>17</sup> were (see the previous section for a brief description), and a value of 11.0 meV was found. These authors are making a systematic study of convergence for a variety of calcula-

tional levels. Junker and Huang<sup>41</sup> in a calculation using complex-coordinate methods have deduced a natural width of 12.1 meV. An extension to this work by Junker<sup>42</sup> has given 12.55 and 11.72 meV for two target wave functions with differing amounts of correlation.

During the course of the present study, a search was made immediately above the  $^2S$  resonance for structure which has been reported by Kuyatt *et al.*,<sup>43</sup> Gibson and Dolder,<sup>36</sup> Golden and Zecca,<sup>35</sup> and Golden *et al.*<sup>28</sup> Such structure has been assumed to represent a narrow  $p$ -wave resonance, but Andrick and Langhans<sup>44</sup> have pointed out that the profile seen by Golden *et al.*<sup>28</sup> has the wrong asymmetry for a  $p$ -wave resonance. The Andrick and Langhans<sup>44</sup> measurements with 40-meV resolution and  $3 \times 10^8$  counts/channel place upper

limits on the widths of any resonances in this region to 10  $\mu$ eV for  $p$ -wave and 30  $\mu$ eV for  $s$ -wave resonances. In the present measurements, no structure has been seen in this energy region. Despite the much better resolution, we have not been able to lower the above limits due to the much lower signal level; our results imply upper limits of about 10 and 50  $\mu$ eV, respectively.

#### ACKNOWLEDGMENTS

The authors gratefully acknowledge the experimental work of Dr. James E. Land, and the valuable discussions of theoretical results with Dr. David Norcross. This work was supported by the National Science Foundation through Grant No. PHY76-04761 to the University of Colorado.

\*Present address: Div. 211.06, National Bureau of Standards, Washington, D. C. 20234.

†Staff Member, Quantum Physics Division, National Bureau of Standards.

<sup>1</sup>G. J. Schulz, *Phys. Rev. Lett.* **10**, 104 (1963).

<sup>2</sup>G. J. Schulz, *Rev. Mod. Phys.* **45**, 378 (1973).

<sup>3</sup>D. E. Golden, *Electron and Photon Interactions with Atoms*, edited by H. Kleinpoppen and M. R. C. McDowell (Plenum, New York, 1976), p. 639.

<sup>4</sup>D. Andrick, *Adv. At. Molec. Phys.* **9**, 207 (1973).

<sup>5</sup>A. C. Gallagher and G. York, *Rev. Sci. Instrum.* **45**, 662 (1974).

<sup>6</sup>R. J. Van Brunt and A. C. Gallagher, in *Abstracts of the Tenth ICPEAC, Paris, 1977*, edited by M. Barat and J. Reinhardt (Commissariat a l'Energie Atomique, Paris, 1977), p. 940.

<sup>7</sup>R. J. Van Brunt and A. C. Gallagher, in *Electronic and Atomic Collisions*, edited by G. Watel (North-Holland, Amsterdam, 1978).

<sup>8</sup>F. Rosebury, *Handbook of Electron Tube and Vacuum Techniques* (Addison-Wesley, Reading, Mass., 1965).

<sup>9</sup>J. N. H. Brunt, G. C. King, and F. H. Read, *J. Phys. B* **10**, 1289 (1977).

<sup>10</sup>J. Comer and F. H. Read, *J. Phys. B* **4**, 1055 (1971).

<sup>11</sup>P. J. Chantry, *J. Chem. Phys.* **55**, 2746 (1971).

<sup>12</sup>N. F. Mott and H. S. W. Massey, *The Theory of Atomic Collisions* (Oxford University Press, London and New York, 1965).

<sup>13</sup>U. Fano, *Phys. Rev.* **124**, 1866 (1961).

<sup>14</sup>J. F. Williams, *J. Phys. B* **12**, 265 (1979).

<sup>15</sup>D. Andrick and A. Bitsch, *J. Phys. B* **8**, 393 (1975).

<sup>16</sup>R. K. Nesbet, *J. Phys. B* **12**, L243 (1979); *Phys. Rev. A* **20**, 58 (1979).

<sup>17</sup>G. Foster, D. G. Hummer, and D. W. Norcross, *Bull. Am. Phys. Soc.* **24**, 1183 (1979).

<sup>18</sup>D. G. Thompson, *Proc. R. Soc. London Ser. A* **294**, 160 (1966).

<sup>19</sup>P. J. Leonard and J. A. Barker, in *Theoretical Chemistry, Advances and Perspectives*, edited by H. Eyring and D. Henderson (Academic, New York, 1975), Vol.

1, p. 117.

<sup>20</sup>T. F. O'Malley, L. Rosenberg, and L. Spruch, *Phys. Rev.* **125**, 1300 (1961).

<sup>21</sup>A. L. Sinfailam and R. K. Nesbet, *Phys. Rev. A* **6**, 2118 (1972).

<sup>22</sup>D. W. Marquardt, *J. Soc. Ind. Appl. Math.* **11**, 431 (1963). The code used was from *STATLIB: A Library of FORTRAN Subroutines for Statistical Analysis of Experimental Data* by P. V. Tryon and J. R. Donaldson (National Bureau of Standards, Center for Applied Mathematics, Statistical Engineering Laboratory, Boulder, Colorado, 1963).

<sup>23</sup>N. C. Steph, L. McDonald, and D. E. Golden, *J. Phys. B* **12**, 1507 (1979).

<sup>24</sup>D. F. Register, S. Trajmar, and S. K. Srivastava, *Phys. Rev. A* **21**, 1134 (1980).

<sup>25</sup>J. A. Preston, M. A. Herides, and J. W. McConkey, *J. Phys. E* **6**, 661 (1973).

<sup>26</sup>J. W. McConkey and J. A. Preston, *J. Phys. B* **8**, 63 (1975).

<sup>27</sup>S. Cvejanović, J. Comer, and F. H. Read, *J. Phys. B* **7**, 468 (1974).

<sup>28</sup>D. E. Golden, F. D. Schowengerdt, and J. Macek, *J. Phys. B* **7**, 478 (1974).

<sup>29</sup>D. Roy, A. Delage, and J. -D. Carette, *J. Phys. E* **8**, 109 (1975).

<sup>30</sup>J. F. Williams and B. A. Willis, *J. Phys. B* **7**, L51 (1974); **7**, L56 (1974).

<sup>31</sup>T. F. O'Malley, P. G. Burke, and K. A. Berrington, *J. Phys. B* **12**, 953 (1979).

<sup>32</sup>R. E. Kennerly and R. A. Bonham, *Phys. Rev. A* **17**, 1844 (1978).

<sup>33</sup>T. S. Stein, W. E. Kauppila, V. Pol, J. H. Smart, and G. Jesion, *Phys. Rev. A* **17**, 1600 (1978).

<sup>34</sup>J. A. Simpson and U. Fano, *Phys. Rev. Lett.* **11**, 158 (1963).

<sup>35</sup>D. E. Golden and A. Zecca, *Rev. Sci. Instrum.* **42**, 210 (1971).

<sup>36</sup>J. R. Gibson and K. T. Dolder, *J. Phys. B* **2**, 741 (1969).

- <sup>37</sup>D. Andrick and H. Ehrhardt, *Z. Phys.* **192**, 99 (1966).
- <sup>38</sup>H. Ehrhardt, L. Langhans, and F. Linder, *Z. Phys.* **214**, 179 (1968).
- <sup>39</sup>J. Comer and F. H. Read, *J. Electron Spectrosc. Relat. Phenom.* **2**, 87 (1973).
- <sup>40</sup>V. A. Hazi, *J. Phys. B* **11**, L259 (1978).
- <sup>41</sup>B. R. Junker and C. L. Huang, *Phys. Rev. A* **18**, 313 (1978).
- <sup>42</sup>B. R. Junker, *Phys. Rev. A* **18**, 2437 (1978).
- <sup>43</sup>C. E. Kuyatt, J. A. Simpson, and S. R. Mielczarek, *Phys. Rev.* **138**, A385 (1965).
- <sup>44</sup>D. Andrick and L. Langhans, *J. Phys. B* **8**, 1245 (1975).
- <sup>45</sup>J. Calloway, R. W. Labahu, R. T. Poe, and W. M. Duxler, *Phys. Rev.* **168**, 12 (1968).
- <sup>46</sup>P. S. Hooper, W. Franzen, and R. Gupta, *Phys. Rev.* **168**, 50 (1968).
- <sup>47</sup>W. M. Duxler, R. T. Poe, and R. W. Labahn, *Phys. Rev. A* **4**, 1935 (1971).
- <sup>48</sup>P. G. Burke and W. D. Robb, *J. Phys. B* **5**, 44 (1972).
- <sup>49</sup>B. S. Yarlagadda, G. Csanak, H. S. Taylor, B. Schneider, and R. Yaris, *Phys. Rev. A* **7**, 146 (1973).
- <sup>50</sup>Quoted in Ref. 3 as being in S. Ormonde and D. E. Golden, *Phys. Rev. Lett.* **31**, 1161 (1973), although we have not found a value quoted there.
- <sup>51</sup>E. Wickmann and P. Heiss, *J. Phys. B* **7**, 1042 (1974).
- <sup>52</sup>R. K. Nesbet, *Phys. Rev. A* **12**, 444 (1975).
- <sup>53</sup>J. Hata, *J. Chem. Phys.* **66**, 1266 (1977).
- <sup>54</sup>K. L. Kwok and F. Mandl, *Proc. Phys. Soc. London* **86**, 501 (1965).
- <sup>55</sup>P. G. Burke, J. W. Cooper, and S. Ormonde, *Phys. Rev.* **183**, 245 (1969).
- <sup>56</sup>D. E. Golden and A. Zecca, *Phys. Rev. A* **1**, 241 (1970).
- <sup>57</sup>A. Temkin, A. K. Bhatia, and J. N. Bardsley, *Phys. Rev. A* **5**, 1663 (1972).
- <sup>58</sup>R. A. Bain, J. N. Bardsley, B. R. Junker, and C. V. Sukumar, *J. Phys. B* **16**, 2189 (1974).
- <sup>59</sup>I. R. Barden, C. Bottcher, and K. R. Schneider, *J. Phys. B* **8**, L1 (1975).
- <sup>60</sup>K. A. Berrington, P. G. Burke, and A. L. Sinfailam, *J. Phys. B* **8**, 1459 (1975).